IL NUOVO CIMENTO Vol. 36 C, N. 1 Suppl. 1 Gennaio-Febbraio 2013
DOI 10.1393/ncc/i2013-11493-6

Colloquia: 12th Italian-Korean Symposium 2011

Einstein is still right: New tests of gravitational dynamics in the field of the Earth

R. Peron

Istituto di Astrofisica e Planetologia Spaziali, Istituto Nazionale di Astrofisica, IFSI/INAF
Via del Fosso del Cavaliere 100, 00133 Roma, Italy

ricevuto il 9 Marzo 2012

Summary. — It is presented and discussed here a recent analysis of LAGEOS II laser tracking data, which led to the first direct verification of the gravitoelectric relativistic precession in the field of the Earth, and to the simultaneous measurement of the Lense-Thirring and de Sitter effects. Emphasis is given on the analysis strategy and the modelization issues. It is also shown a further result, consisting in a new limit, much more stringent than the previous ones, on a possible non-Newtonian (Yukawa-like) interaction, acting at the scale of the system semimajor axis.

PACS 04.80.Cc – Experimental tests of gravitational theories.
PACS 91.10.Sp – Satellite orbits.
PACS 95.10.Eg – Orbit determination and improvement.
PACS 95.40.+s – Artificial Earth satellites.

1. – Introduction

After almost a century since its development by Albert Einstein, the theory of general relativity continues to be a pillar for our knowledge of the physical world. Despite decades of experimental tests and evidence of various nature, challenges are put on it, from laboratory to cosmological scales. On this respect, tests performed in the Solar System are an important tool; they allow verifying predictions of the theory and placing contraints on alternative theories (for a recent review, see [1]). Perhaps not surprisingly, important tests can be performed in the vicinity of the Earth, in the conditions of weak-field and slow motion, using techniques borrowed from space geodesy. In fact several geodynamic satellites, developed for geodetic and geophysical purposes, orbit around Earth. They are tracked using the high-precision technique of Satellite Laser Ranging (SLR) [2], enabling very accurate reconstruction of their orbits. Among these, the LAGEOS satellites [3], thanks to their physical characteristics and orbit, are the best suited for fundamental physics tests.

LAGEOS (launched in 1976) and LAGEOS II (launched in 1992) are the best man-made realization of a gravitational test mass, *i.e.* of an object that ideally does not perturb the gravitational field in which it moves. Following the description of gravitational (spacetime) dynamics provided by the theory of general relativity, they should undergo geodetic motion in the spacetime curved by Earth mass-energy and angular momentum [4]. The deviations from the motion predicted by Newtonian dynamics are small, but can be detected thanks to the high precision of SLR. The main issue to be faced is the precise modeling of the satellite dynamics. Indeed, several contributions both of gravitational and non-gravitational origin are at work in shaping its motion. Precise models for most of them are available, down to the required accuracy level. A precise orbit determination and parameter estimation procedure is required in order to reconstruct a satellite orbit from tracking data; residuals time series can then be obtained, and the signature of the sought for effects could be recovered.

In the past years a lot of effort has been put in performing dedicated analyses of LAGEOS and LAGEOS II tracking data to extract the relativistic signals. This led to the first direct evidence of the Lense-Thirring effect on orbiting test masses [5-7] and to the first direct measurement of "Einstein" or "Schwarzschild" gravitoelectric precession in the field of the Earth [8], following a suggestion of [9]. In particular, this most recent work dealt with the LAGEOS II argument of perigee as the fundamental observable from which to extract a wealth of information related to relativistic dynamics and to possible alternative phenomenology, as it is shown in the following.

2. – Relativistic effects on test masses around Earth

General relativity, in its weak-field and slow-motion limit, provides an effective description of the gravitational phenomena around Earth. A formulation of the relevant equations of motion in a geocentric non-inertial reference system (non-rotating with respect to the barycentric one) is given in [10], from which we quote the relevant terms. The analysis here described is consistent with this formulation.

A test mass orbiting around Earth is subject in its motion to three main relativistic effects. The biggest contribution comes from the gravitoelectric curvature of spacetime induced by Earth mass-energy:

$$\mathbf{a}_{Schw} = \frac{Gm_E}{c^2 r^3}\left[\left(\frac{4Gm_E}{r} - v^2\right)\mathbf{r} + 4(\mathbf{v}\cdot\mathbf{r})\mathbf{v}\right]. \tag{1}$$

The satellite, in its motion around Earth, follows its revolution in the spacetime curved by the Sun mass-energy; this (via parallel transport of the normal to the satellite orbit) induces the *geodetic* or *de Sitter precession*:

$$\mathbf{a}_{dS} = 2\boldsymbol{\Omega}\times\mathbf{v}, \qquad \boldsymbol{\Omega} \approx -\frac{3}{2}(\mathbf{V}_E - \mathbf{V}_S)\times\frac{GM_S\mathbf{X}_{ES}}{c^2 R_{ES}^3}. \tag{2}$$

In general relativity, unlike Newtonian physics, mass-energy currents also cause effects, named gravitomagnetic (see [4]). In particular, Earth intrinsic angular momentum curves spacetime and induces a further effect on the satellite orbit, called *Lense-Thirring effect* (also termed *dragging of inertial frames* in a more general setting):

$$\mathbf{a}_{LT} = \frac{2Gm_E}{c^2 r^3}\left[\frac{3}{r^2}(\mathbf{r}\times\mathbf{v})(\mathbf{r}\cdot\mathbf{J}) + \mathbf{v}\times\mathbf{J}\right]. \tag{3}$$

TABLE I. – *Rate and orbital shift of the different types of secular relativistic precession on LAGEOS II argument of perigee, and their sum* ($1\,\mathrm{mas/y} = 1$ *milliarcsecond per year*).

Precession	Rate [mas/y]	Shift [m]
$\Delta\dot{\omega}^{Schw}$	3351.95	7.61
$\Delta\dot{\omega}^{dS}$	10.69	$2.44 \cdot 10^{-2}$
$\Delta\dot{\omega}^{LT}$	−57.00	$-1.29 \cdot 10^{-1}$
$\Delta\dot{\omega}^{rel}$	3305.64	7.51

In the notation we follow [10]. In particular, c is the speed of light, G the Newtonian gravitational constant, m_E and J are Earth mass and angular momentum, $\mathbf{r}$ and $\mathbf{v}$ the test mass position and velocity in the geocentric frame, M_S is the Sun mass, $\mathbf{V}_E$ and $\mathbf{V}_S$ are the Earth and Sun geocentric positions, $\mathbf{X}_{ES}$ is the geocentric Earth-Sun vector, with distance R_{ES}. We notice that, while the effects described by eqs. (1) and (3) depend only on the Earth mass-energy and angular momentum, the geodetic precession of eq. (2) involves also the Sun (relativistic three-body problem)([1]).

Using the methods of celestial mechanics, the effects of relativistic corrections in the satellite Keplerian elements can be evaluated. It turns out that the argument of perigee is a good observable to see in action all three. Given its higher orbital eccentricity (~ 0.014 compared to ~ 0.004) LAGEOS II is more suited than LAGEOS for performing such a measurement. Using perturbation theory, the argument of perigee secular precession can be calculated for the three effects; see the second column of table I (and [8]). The dominant effect is the gravitoelectric precession, analogous to Mercury perihelion precession in the field of the Sun, with smaller contributions from geodetic and gravitomagnetic effects. Are the expected values compatible with the uncertainty associated to tracking data? An estimate of the orbital shift due to each effect can be obtained for nearly circular orbits by $\Delta x|_{14d} \simeq a\Delta\alpha|_{14d}$; here a is the semimajor axis of LAGEOS II orbit ($a \simeq 1.22 \cdot 10^7$ m) and $\Delta\alpha$ is the precession integrated over the 14 days estimation period (see sect. **4**). The values can be seen in the third column of table I: given a typical SLR normal point precision of $\simeq 1$ cm, the gravitoelectric signal is well above the noise, while the geodetic and gravitomagnetic ones are barely above it([2]).

3. – Testing inverse-square law

Tests for the inverse-square law behaviour of gravitation, in the Newtonian limit, are an important issue. On one side they are useful to better characterize gravitation itself, especially in the short and intermediate range. On another side, possible violations of this behaviour could be related to new interactions between bodies acting at macroscopic distances. Usually this is modeled via a Yukawa-type potential added to the Newtonian

([1]) This effect appears due to the chosen geocentric non-inertial reference system.
([2]) In any case, the secular, "systematic" character of the relativistic signals causes them to appear from the noise upon integration on a sufficiently long time.

one, such that between two bodies of masses m_1 and m_2, respectively, at distance r apart

$$V = -G_\infty \frac{m_1 m_2}{r}\left(1 + \alpha e^{-r/\lambda}\right). \tag{4}$$

Here the Yukawa-type part has a characteristic range λ([3]) beyond which it becomes negligible, and a relative strength α with respect to the Newtonian part; G_∞ is the Newtonian constant of gravitation in the limit $r \to \infty$. The suggestion in the eighties of a possible "fifth force" [11] boosted further research on this (see also [12, 13] for reviews and [14] for recent results).

An adequate observable in order to test for such non-Newtonian behaviour is the pericenter of a binary system. A perturbative analysis of pericenter shift has been performed in [15]. The effect is maximum at a scale comparable with the system semimajor axis; therefore, in the Earth-LAGEOS II case, the experiment would be sensitive mainly to an interaction with $\lambda = a$ (a being the semimajor axis of LAGEOS II orbit).

4. – Measurement concept and strategy

The core of the measurement is a precise orbit determination of LAGEOS II, in which the SLR normal points are fitted with suitable models for satellite dynamics, measurement procedure and reference frames. The outcome of such a procedure, apart from the precise orbit and the estimate of selected parameters, is a set of time series for Keplerian elements residuals, from which to seek for a signature of the relativistic effects. The software used for the analysis is GEODYN II (NASA GSFC) [16].

SLR is one of the most powerful and precise among the tracking techniques. A laser pulse is sent from an Earth-bound station to the satellite, where it is reflected back in the same direction from cube-corner retroreflectors and received at the station. The two-way time of flight is measured, and from it the instantaneous station-satellite distance (*range*) is recovered. The random error of raw observations is lowered by forming the so-called *normal points*, *i.e.* suitably averaged ranges over fixed time intervals (bins). The typical error of normal points for LAGEOS satellites is below the cm. Laser range observations from the various stations on the globe are collected by the International Laser Ranging Service (ILRS) [2] and are publicly available.

The tracking data contain information related to the relativistic dynamics of satellites, but this information is mixed with all the other dynamics. In order to extract it, a multi-arc technique has been employed [17]. The time period considered in the data analysis has been divided into shorter periods, called *arcs*, 15 days long. For each arc the tracking data are reduced, resulting in an estimate of the state vector (position and velocity) at the beginning of the arc and of selected parameters for the dynamics. A very precise orbit is therefore obtained for each arc, which can be expressed in terms of Keplerian elements. The arcs have a 1 day overlap; calculating the difference in elements at the middle of this overlap provides time series of *residuals* which contain information on the part of dynamics which has not been modeled (or has been mismodeled). The fundamental observable being the range, strictly also the residuals, in their meaning of "observed" - "calculated", are ranges. The elements difference method used in this analysis retains the concept for the various Keplerian elements, as shown in [18]. Analysis of the residuals

([3]) Corresponding to a field of mass $m = \hbar/\lambda c$.

TABLE II. – *Modeling setup used in the analysis. Included are models for gravitational and non-gravitational perturbations, and for reference frames respectively.*

Model for	Model type	Reference
Geopotential (static)	EIGEN-GRACE02S	[19]
Geopotential (time-varying, tides)	Ray GOT99.2	[20]
Geopotential (time-varying, non-tidal)	IERS Conventions (2003)	[21]
Third body	JPL DE-403	[22]
Relativistic corrections	Parametrized post-Newtonian	[10]
Direct solar radiation pressure	Cannonball	[16]
Earth albedo	Knocke-Rubincam	[23]
Station positions	ITRF 2000	[24]
Ocean loading	Schernek and GOT99.2	[16, 20]
Earth Rotation Parameters	IERS EOP C04	[25]

time series allows recovering *a posteriori* the signature of effects which have not been modeled, as it was purposedly done for the relativistic part.

The strategy employed in this analysis could be considered as "minimal" or "conservative" in the following sense. The precise modeling of LAGEOS II orbit requires complex models, which depend on thousands of parameters (see sect. **5**). While in geodynamical and geophysical problems the majority of them could be estimated, in our case only few of them were; the remaining ones were treated as *consider parameters*, *i.e.* parameters which are already known with sufficient accuracy from other sources. This considerably simplifies the mathematical structure of the problem being solved and strongly lowers the chance of estimation biases.

5. – Models for precise orbit determination

The procedures for determining the satellite orbit at a level comparable with the quality of tracking data require models not only for satellite dynamics, but also for measurement procedure and reference frame transformations. These (see table II) are briefly summarized in the following. It has to be remarked that, in general, the analysis here described is consistent with the IERS Conventions (2003) [21](4).

A first class of perturbations is related to gravitational effects. The Earth is not a perfect sphere, and the deviations of its gravitational field from the point mass one, due to the inhomogeneous mass density distribution, are by far the most important source of perturbations in the orbit of satellites. It is customary in geodesy and geophysics to represent the gravitational potential energy per unit mass by expanding it in spherical

(4) IERS (International Earth Rotation Service) is the international organization in charge of maintaining the reference frames used in astronomy, geodesy and geophysics.

harmonics $Y_{\ell,m}(\theta,\phi)$ (real basis, with the superscripts C and S denoting the cosine and sine parts, respectively):

$$U(\mathbf{r}) = -\frac{GM}{r}\left[1+\sum_{l=1}^{\infty}\left(\frac{R}{r}\right)^{l}\sum_{m=0}^{l}(\bar{C}_{lm}Y_{lm}^{C}(\theta,\phi)+\bar{S}_{lm}Y_{lm}^{S}(\theta,\phi))\right]; \tag{5}$$

see for example [26-28]. Here r, θ and ϕ represent the polar coordinates of the point at which the potential U is evaluated; G is the Newtonian gravitational constant, M the Earth mass, R the Earth mean equatorial radius. The normalized coefficient $\bar{C}_{\ell,m}$ and $\bar{S}_{\ell,m}$, with ℓ called *degree* and m *order*, are function of the mass density distribution, and completely characterize the gravitational potential outside the distribution itself. In practice, the series is truncated at some finite ℓ_{max}: the model is then sensitive to inhomogeneities down to the scale $\pi R/\ell_{max}$. Of paramount importance in our analysis are the so-called *zonal* harmonics, *i.e.* those with $m = 0$. In particular, the quadrupole coefficient $\bar{C}_{20}$ has been found to be the major source of uncertainty in the experiment [15]. In our analysis it has been used EIGEN-GRACE02S [19], derived from data of the GRACE mission, to model the geopotential.

The Earth gravitational field, also seen in an "Earth fixed" frame, is not static: it varies in time due to a series of phenomena, from tides to mass transport in the Earth/atmosphere system at various scales. Both solid Earth and ocean tides have been modeled, together with selected non-tidal phenomena (linearly time-varying lower degree zonal harmonics).

The effect of third-body perturbations has been modeled as well, using the well-established Solar System ephemerides by JPL (in our case, DE-403 [22]). As discussed in sect. **2**, the relativistic corrections are consistent with the formulation of [10]. In line with the chosen strategy of recovering the relativistic effects *a posteriori* in the residuals time series, in fact these corrections have been not included in the setup.

A second class of perturbations is given by the non-gravitational effects. These, of various origin, are caused by the interaction of the satellite body with the near-Earth radiation and particle environment. Such forces are typically surface ones and depend in a complex way on the physical properties of the satellite, as well as on its attitude. Even for very simple satellites such as the LAGEOS, spherical in shape, very dense and passive, these effects are relevant and, especially, very difficult to model. A wide literature exists on the subject; we refer to [29-31].

The most important non-gravitational effect is the *direct solar radiation pressure*. This is caused by photons from the Sun being reflected-diffused-absorbed by the satellite surface, resulting in a net momentum transfer to the satellite itself. The resultant acceleration, for a body of spherical shape, is given by

$$\mathbf{a}_{\odot} = -C_R\frac{A\Phi_{\odot}}{mc}\left(\frac{1AU}{r}\right)^{2}\mathbf{s}, \tag{6}$$

where A is the cross-sectional area of the satellite, m its mass, $\Phi_{\odot}$ the solar radiation flux at 1 AU, c the speed of light, r the Sun-satellite distance, $\mathbf{s}$ the Sun-satellite unit vector and C_R (called *radiation coefficient*) summarizes the optical properties of the satellite surface. For LAGEOS II, with $C_R = 1.12$, $a_{\odot} \simeq 3\cdot 10^{-9}\,\mathrm{m/s^2}$. The model expressed by eq. (6) is rather good for the LAGEOS satellites, provided an estimate is done of the

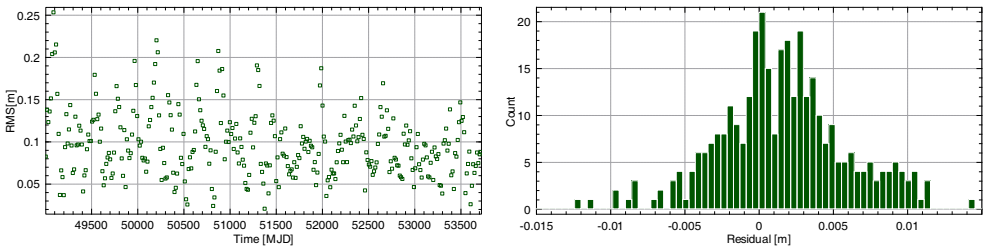

Fig. 1. – Post-fit weighted RMS (left) and residuals in range (right) computed for each of the arcs into which the analysed time period has been divided.

C_R parameter. Evidences have been provided that LAGEOS II optical properties could have been changed since the launch time [32].

6. – Data reduction and results

Thirteen years of LAGEOS II laser tracking data, provided by ILRS [2], have been analyzed. As explained in sect. **4**, for each arc the data have been reduced using the GEODYN II software, obtaining a very precise trajectory. The models employed (see table II) enabled a very good fit of the data, as can be seen in the statistics. In particular, in fig. 1 the post-fit weighted RMS and a histogram of the residuals in range are shown. The average RMS is somewhat higher than the "ideal" level that could be expected based on data quality: this is due to the fact that no relativistic effects were inserted in the modelization set, thereby lowering the overall accuracy. In this way, however, the residuals contain useful information, which is indeed related to relativity itself. This can be seen in the histogram of the residuals in range: their distribution appears close to but is not exactly Gaussian, indicating that some information is still present in the residuals themselves.

The fitted trajectory from the orbit determination allows computing the residuals for each Keplerian element. Here we are interested in those of the argument of perigee, which should contain a signature of all the three relativistic effects discussed in sect. **2**. Due to the secular character of the sought for effects, it is useful to consider not the residuals time series, but the integrated (in time) one, in order to enhance the accumulation of the signal. This can be seen in fig. 2. Two things are apparent from the plot. First, a secular trend, mainly due to the relativistic effects. Second, periodic contributions, mainly due to non-gravitational effects, in particular the Yarkovsky-Schach one (as confirmed by an analysis of the frequencies([5]), see [8]). A fit gives the value $\Delta\dot{\omega}^{meas} = 3306.58\,\mathrm{mas/yr}$ for the slope. This value can be taken as an estimate of the total relativistic perigee precession, given by

$$\Delta\dot{\omega}^{rel} \simeq \epsilon_E \Delta\dot{\omega}^E + \epsilon_{LT}\Delta\dot{\omega}^{LT} + \epsilon_{dS}\Delta\dot{\omega}^{dS}, \tag{7}$$

which according to the theory sums to $\Delta\dot{\omega}^{rel} = 3305.64\,\mathrm{mas/yr}$ (see table I). The slope estimate has small variations depending on the number of periodic effects which are fitted

([5]) The main spectral lines being at about 257 d, 624 d, 485 d and 312 d, respectively.

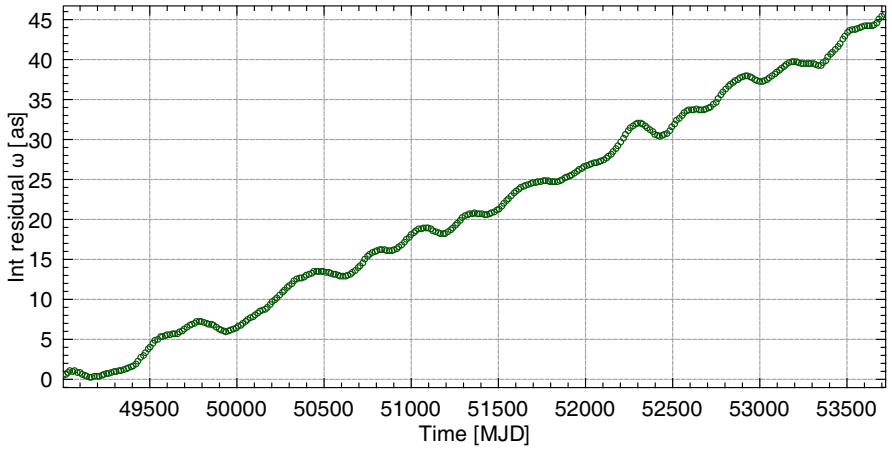

Fig. 2. – Time series of the argument of perigee integrated residuals (1 as = 1 arcsecond). A secular trend is apparent from the plot. Periodic contributions are superimposed on it, mainly of non-gravitational origin.

together with the linear trend. In [8] it has been given the following conservative result for the magnitude of the total relativistic effect, at the post-Newtonian level:

$$\epsilon_\omega = 1 + (0.28 \pm 2.14) \times 10^{-3}, \tag{8}$$

where $\epsilon_\omega = 1$ in general relativity. Since the dominant contribution in eq. (7) comes from

$$\epsilon_E = \frac{2 + 2\gamma - \beta}{3}\,, \tag{9}$$

the estimate given by eq. (8) is mainly a measurement of such a combination of γ and β PPN parameters. This estimate is, to our knowledge, the most accurate measurement for pericenter precession in the field of the Earth ever made. A preliminary error budget for the measurement, taking into account the various systematic errors, estimated the error to be at 2% level [15].

The measured value for argument of perigee precession can also be used to constrain a non-Newtonian contribution to the satellite dynamics, as discussed in sect. **3**. Indeed, the absence of such a signal in the residuals time series allows placing a strong constraint to the strength α at $\lambda = a$. In [8] it has been obtained the following upper bound:

$$|\alpha| \simeq |(1.0 \pm 8.9)| \times 10^{-12}, \tag{10}$$

a huge improvement with respect to previous constraints at this scale and comparable with the Lunar Laser Ranging results.

7. – Conclusion

The availability of a good test mass such as the LAGEOS II satellite, with its associated SLR tracking data, opened up the possibility of performing very precise tests of the

gravitational dynamics in the near-Earth environment, via a precise orbit determination and parameter estimation procedure. The key to such tests are accurate models for the satellite dynamics, as well as for measurement procedure and reference frames. Two important measurements have been described. The first is the simultaneous measurement of all the three main relativistic effects acting on the argument of perigee, providing also a measurement of a combination of the γ and β PPN parameters. The second is a strong constraint on a possible non-Newtonian, Yukawa-like, interaction acting at a range comparable with the system semimajor axis, providing a major improvement with respect to previous measurements.

* * *

The author acknowledges the ILRS for providing high-quality laser ranging data of the LAGEOS II satellite. He also thanks Prof. Remo Ruffini for his kind invitation to the ICRANet 12th Italian-Korean Symposium on Relativistic Astrophysics.

REFERENCES

[1] Will C. M., *Living Rev. Relat.*, **9** (2006) 3.
[2] Pearlman M. R., Degnan J. J. and Bosworth J. M., *Adv. Space Res.*, **30** (2002) 135, doi:10.1016/S0273-1177(02)00277-6.
[3] Cohen S. C. and Smith D. E., *J. Geophys. Res.*, **90** (1985) 9217, doi:10.1029/JB090iB11p09217.
[4] Ciufolini I. and Wheeler J. A., *Gravitation and Inertia* (Princeton University Press, Princeton) 1995.
[5] Ciufolini I., Pavlis E., Chieppa F., Fernandes-Vieira E. and Perez-Mercader J., *Science*, **279** (1998) 2100, doi:10.1126/science.279.5359.2100.
[6] Ciufolini I. and Pavlis E. C., *Nature*, **431** (2004) 958, doi:10.1038/nature03007.
[7] Ciufolini I., Pavlis E. C. and Peron R., *New Astron.*, **11** (2006) 527, doi:10.1016/j.newast.2006.02.001.
[8] Lucchesi D. M. and Peron R., *Phys. Rev. Lett.*, **105** (2010) 231103, doi:10.1103/PhysRevLett.105.231103.
[9] Rubincam D. P., *Celest. Mech.*, **15** (1977) 21, doi:10.1007/BF01229045.
[10] Huang C., Ries J. C., Tapley B. D. and Watkins M. M., *Celest. Mech. Dyn. Astron.*, **48** (1990) 167, doi:10.1007/BF00049512.
[11] Fischbach E., Sudarsky D., Szafer A., Talmadge C. and Aronson S. H., *Phys. Rev. Lett.*, **56** (1986) 3, doi:10.1103/PhysRevLett.56.3.
[12] Fischbach E., Gillies G. T., Krause D. E., Schwan J. G. and Talmadge C., *Metrologia*, **29** (1992) 213, doi:10.1088/0026-1394/29/3/001.
[13] Goldhaber A. S. and Nieto M. M., *Rev. Mod. Phys.*, **82** (2010) 939, doi:10.1103/RevModPhys.82.939.
[14] Gundlach J. H., Schlamminger S. and Wagner T., *Space Sci. Rev.*, **148** (2009) 201, doi:10.1007/s11214-009-9609-3.
[15] Lucchesi D. M., *Phys. Lett. A*, **318** (2003) 234, doi:10.1016/j.physleta.2003.07.015.
[16] Pavlis D. E., *GEODYN Operations Manual* NASA Goddard Contractor Report, SGT, Inc., Greenbelt, MD 2005.
[17] Milani A. and Gronchi G. F., *Theory of Orbit Determination* (Cambridge University Press, Cambridge) 2010.
[18] Lucchesi D. M. and Balmino G., *Plan. Space Sci.*, **54** (2006) 581, doi:10.1016/j.pss.2006.03.001.
[19] Reigber C., Schmidt R., Flechtner F., König R., Meyer U., Neumayer K.-H., Schwintzer P. and Zhu S. Y., *J. Geodyn.*, **39** (2005) 1, doi:10.1016/j.jog.2004.07.001.

[20] Ray R. D., *A Global Ocean Tide Model From TOPEX/POSEIDON Altimetry: GOT99.2*, NASA/TM-1999-209478, 1999.
[21] McCarthy D. D. and Petit G. (Editors), *IERS Conventions (2003)*, IERS Technical Note No. 32, IERS, 2004.
[22] Standish E. M., Newhall X. X., Williams J. G. and Folkner W. M., *JPL Planetary and Lunar Ephemerides, DE403/LE403*, JPL IOM 314.10-127, 1995.
[23] Rubincam D. P., Knocke P., Taylor V. R. and Blackwell S., *J. Geophys. Res.*, **92** (1987) 11662, doi:10.1029/JB092iB11p11662.
[24] Boucher C., Altamimi Z., Sillard P. and Feissel-Vernier M., *The ITRF2000*, IERS Technical Note No. 31, IERS, 2004.
[25] International Earth Rotation Service, *EOP Combined Series EOP C04*.
[26] Bertotti B., Farinella P. and Vokrouhlický D., *Physics of the Solar System* (Kluwer, Dordrecht) 2003.
[27] Hofmann-Wellenhof B. and Moritz H., *Physical Geodesy* (Springer, Berlin) 2006.
[28] Montenbruck O. and Gill E., *Satellite Orbits* (Springer, Berlin) 2000.
[29] Lucchesi D. M., *Plan. Space Sci.*, **49** (2001) 447, doi:10.1016/S0032-0633(00)00168-9.
[30] Lucchesi D. M., *Plan. Space Sci.*, **50** (2002) 1067, doi:10.1016/S0032-0633(02)00052-1.
[31] Milani A., Nobili A. M. and Farinella P., *Non-Gravitational Perturbations and Satellite Geodesy* (Adam Hilger, Bristol) 1987.
[32] Lucchesi D. M., Ciufolini I., Andrés J. I., Pavlis E. C., Peron R., Noomen R. and Currie D. G., *Plan. Space Sci.*, **52** (2004) 699, doi:10.1016/j.pss.2004.01.007.